Hans-F. Graf
Ingo Kirchner
Ingrid Schult

Max-Planck-Institut
für Meteorologie

Alan Robock

Department of Meteorology
University of Maryland
College Park
MD 20742
USA

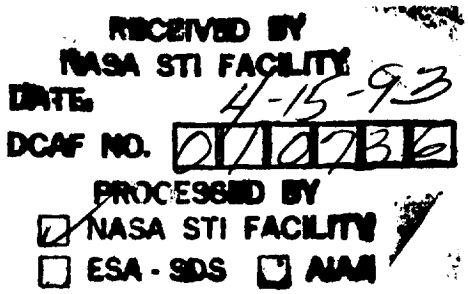

MAX-PLANCK-INSTITUT
FÜR METEOROLOGIE
BUNDESSTRASSE 55
D-2000 HAMBURG 13
F.R. GERMANY

Tel.: +49 (40) 4 11 73-0
Telex: 211092 mpime d
Telemail: MPI.METEOROLOGY
Telefax: +49 (40) 4 11 73-298

Pinatubo Eruption Winter Climate Effects: Model Versus Observations

H.-F. Graf, I. Kirchner, A. Robock* and I. Schult

Max-Planck-Institut für Meteorologie
Bundesstr. 55, 2000 Hamburg 13, Germany
*Department of Meteorology, University of Maryland,
College Park, MD 20742, USA

October 1992

ISSN 0937–1060

Abstract:

Large volcanic eruptions, in addition to the well-known effect of producing global cooling for a year or two, have been observed to produce shorter-term responses in the climate system involving non-linear dynamical processes. In this paper, we use the ECHAM2 general circulation model forced with stratospheric aerosols to test some of these ideas. Run in a perpetual-January mode, with tropical stratospheric heating from the volcanic aerosols typical of the 1982 El Chichón eruption or the 1991 Pinatubo eruption, we find a dynamical response with an increased polar night jet in the Northern Hemisphere (NH) and stronger zonal winds which extend down into the troposphere. The Azores High shifts northward with increased tropospheric westerlies at 60°N and increased easterlies at 30°N. Surface temperatures are higher both in northern Eurasia and North America, in agreement with observations for the NH winters or 1982-83 and 1991-92 as well as the winters following the other 10 largest volcanic eruptions since 1883.

Introduction:

The eruption of Philippine volcano Mt. Pinatubo on June 15, 1991, was possibly the most sulfur-rich of this century, putting about 20 Mt of SO_2 into the Stratosphere (Bluth et al. 1992), which converted to 40 to 50 Mt of sulfuric acid aerosols. Although conventional wisdom holds that volcanic aerosols produce cooling at the surface due to reduction of incoming solar radiation (and indeed that effect is to be expected on a two- to three-year timescale (Robock 1991)), the winter of 1991-92 (DJF) was warmer than average over North America and the Eurasian middle latitudes both in satellite derived temperatures of the lower half of the troposphere and in synoptic surface observations at the same time. Negative temperature anomalies were observed mainly over the eastern Mediterranean and over the northeastern part of North America, the Davis strait and Greenland. The question arises as to whether this anomaly pattern is produced by a deterministic process other than the reduction of shortwave radiation or is simply a manifestation of the internal climate variability. The possibile effect of the coincidence of volcanic aerosol with an El Niño leading to the higher continental winter temperatures is discussed e.g. by Robock (1984) and Graf (1986). Experiments to study this effect in more detail are currently ongoing and will be described in a forthcoming paper.

In the literature some contradictive results have been published about the effect of volcanic aerosol on the climate of the cold season both from model studies and observations. Recent numerical volcano experiments with general circulation models (GCM) (Graf 1992 and Hansen et al. 1992), in which the additional aerosol was introduced implicitly by reducing the solar radiation, shows the strongest climate signal during the warmer seasons. This is not surprising, since the simple linear reduction of incoming solar radiation as used in these studies has only a minor absolute effect in high latitudes during winter. Another experiment, mainly focussed on the stratospheric processes (Rind et al. 1992) and including longwave and shortwave heating, found decreased tropospheric midlatitude westerlies. An energy-balance model (Robock, 1984) and an annual cycle GCM calculation (Hansen et al. 1988, as analyzed by Robock and Liu, in preparation) actually find enhanced cooling in the winter polar regions due to the sea ice / thermal inertia feedback. However there are observational studies that show winter warming after large eruptions over western North America

(Lough and Fritts, 1987) and northern Europe (Groismann 1985, 1992). A reanalysis of global temperature data (Robock and Mao 1992, submitted) reveals winter warming over large parts of Eurasia after all major volcanic eruptions of the last century since the eruption of Krakatau in 1883. The question thus arises, whether there are processes other than the direct effect of radiation which determine the climate response to volcanic aerosol during winter. One possibility is the dynamic coupling of stratosphere and troposphere, as has been shown with simple linear models (Geller and Alpert 1980, Schmitz and Grieger 1980). Numerical experiments (Boville 1986) showed for instance reduced meridional heat transport in the troposphere in the NCAR Climate Community Model for conditions typical for stratospheric westerly circulation (cold polar and warm tropical stratosphere).

We therefore conducted a GCM experiment in which, in addition to the reduction of solar radiation at the top of the model atmosphere, heating rate anomalies were added in the stratosphere producing a rather realistic temperature anomaly field in the stratosphere. We want to study the atmospheric response to the volcanic disturbance keeping the ocean fixed. Therefore any transitional effects from slowly varying parts of the climate system can be neglected. The atmospheric memory is at best two weeks. Since our main interest is in wintertime conditions, the model was integrated in a "Perpetual January"-experiment mode. Cumulative hydrological effects like the build-up of an enhanced snow cover and its effect on the Asian monsoon system are discussed in Graf (1992).

Experimental Setup

The stratospheric aerosol distribution observed in January 1983 in midlatitudes of the northern hemisphere, ten months after the eruption of El Chichón, is very similar to that seven months after Pinatubo in January 1992. The transmission of direct solar radiation for wavelengths of λ=0.3μm to 2.8μm over Mauna Loa (see Climate Diagnostics Bull., June 1992) is somewhat reduced in January 1992 (τ=0.86) compared with January 1983 (τ=0.89), and the column aerosol backscatter coefficient at ruby-wavelength (λ=0.69 μm)at the same place is larger by a factor of two for January 1992. But, in middle latitudes of the northern hemisphere, lidar measurements of the aerosol column backscatter are comparable for both Januaries (Jäger, pers. comm., see Figure 1). Later in 1992 the Pinatubo aerosol became more effective in

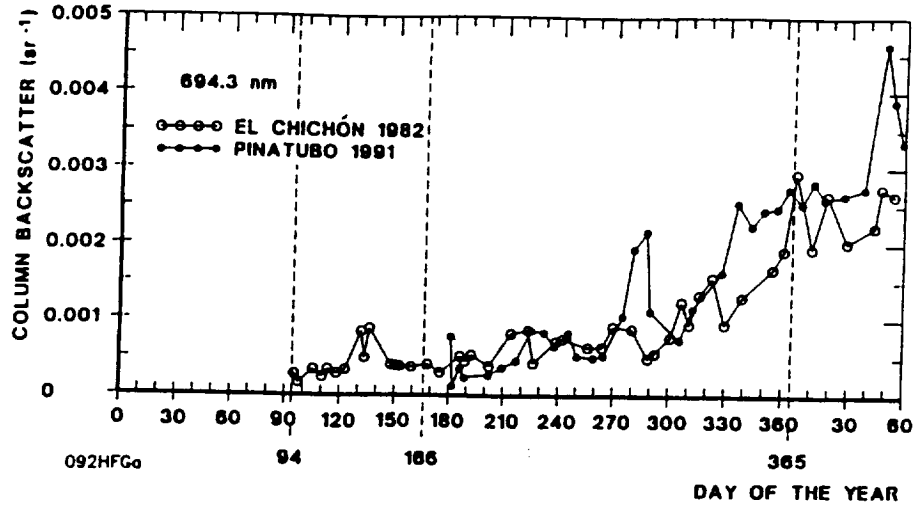

Figure 1: Column backscatter for λ=694.3 nm, Lidar observations over Garmisch-Partenkirchen (47.5°N, 11.0°E) after the eruption of El Chichón, April 4, 1982 (open circles) and Pinatubo, June 15, 1991 (full circles) (from Jäger, 1992, extended and redrawn). Day of Year 94 (166) is the day of the respective eruption

extinguishing solar radiation also in midlatitudes by a factor of 2 to 3 compared to the El Chichón aerosol. For our model simulation we used a prescribed aerosol distribution according to January 1992 observations, i.e. similar aerosol like in January 1983 for midlatitudes and stronger aerosol in low latitudes leading to a reduction in shortwave radiation as shown in Figure 2 (dashed line). Lacis et al. (1992) found that the only important parameter for the net radiative forcing due to volcanic stratospheric aerosol is the optical depth. Therefore, lacking further detailed information about the optical properties of the January 1992 aerosol (like

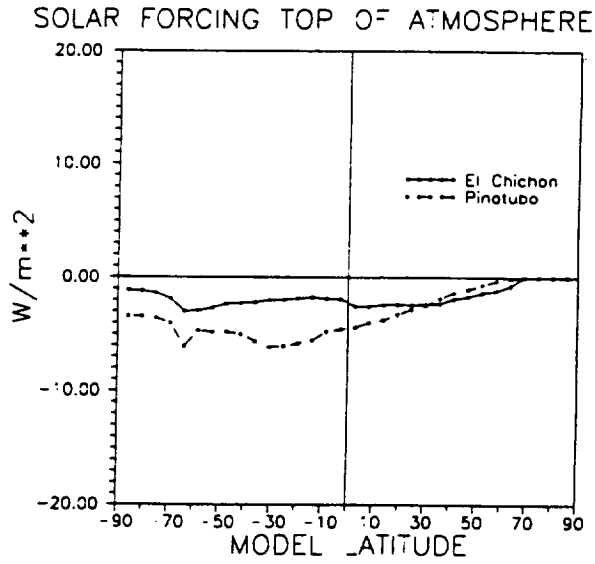

Figure 2: Reduction of solar radiation [W/m²] due to volcanic aerosol for January 1983 (solid line) and 1992 (broken line). The January 1992 values are used as solar forcing in the experiments.

e.g. effective radii of the particles), we used model calculations based on El Chichón to prescribe these.

The climate model used in our computations is the ECHAM2 GCM, used at the Max-Planck-Institute für Meteorologie for climate modelling research (Roeckner et al. 1992). We used the T21 version (horizontal resolution approximately 5.6°) with 19 vertical levels, the full diurnal cycle and standard physics, including cloud-radiation interactions. Sea surface temperature (SST) and sea ice extent are prescribed from climatology. An investigation of the relative effects of anomalous SST assiociated with the 1991-92 El Niño and the volcanic aerosol is in preparation.

Since the radiation scheme of the ECHAM2 climate model is unable to deal with variable aerosol concentrations, we decided to use the "anomaly forcing" technique which has previously been used to study the climate response to the smoke from the burning Kuwait oil wells (Bakan et al. 1991). This technique allows the inclusion of any radiational effects of trace gases or aerosols in the model by the use of an additional radiation model, which explicitely treats the species under investigation. In this case we used the δ-Eddington model, Bakan (1982), with the extensions for aerosol and ozone from Schult (1991). We ran this model parallel to the original ECHAM2 radiation code once with and once without the prescribed aerosol with the atmospheric conditions from the climate model. The flux differences of the two δ-Eddington computations arethen added to the results of the original code. After six months of running this complete interactive radiation and circulation code we obtained mean monthly anomalies of the radiative fluxes and heating rates. The effect of the aerosol longwave radiation on the surface radiation balance was more than one order of magnitude less than the total effect. It will therefore (also in accordance with Lacis et al. 1992) be neglected in the computations described below.

Since the fully interactive model increases the computation time for ECHAM2 by a factor of five, we avoided its explicit application in order to be able to run a series of experiments long enough for statistical investigations. Thus, we used the externally computed mean heating rate anomaly and the mean reduction of the shortwave radiation (Figures 2a and 3) of the fully interactive model for a series of perpetual January simulations. The

model was initiated with data from one arbitrarily chosen January 1 of the control experiment and integrated for 30 days. Doing this 60 times (each new 1st January being initialized with the fields of the 30th January of the former integration) we produced a series of 60 January simulations both for the disturbed (Experiment) and the undisturbed (Control) case.

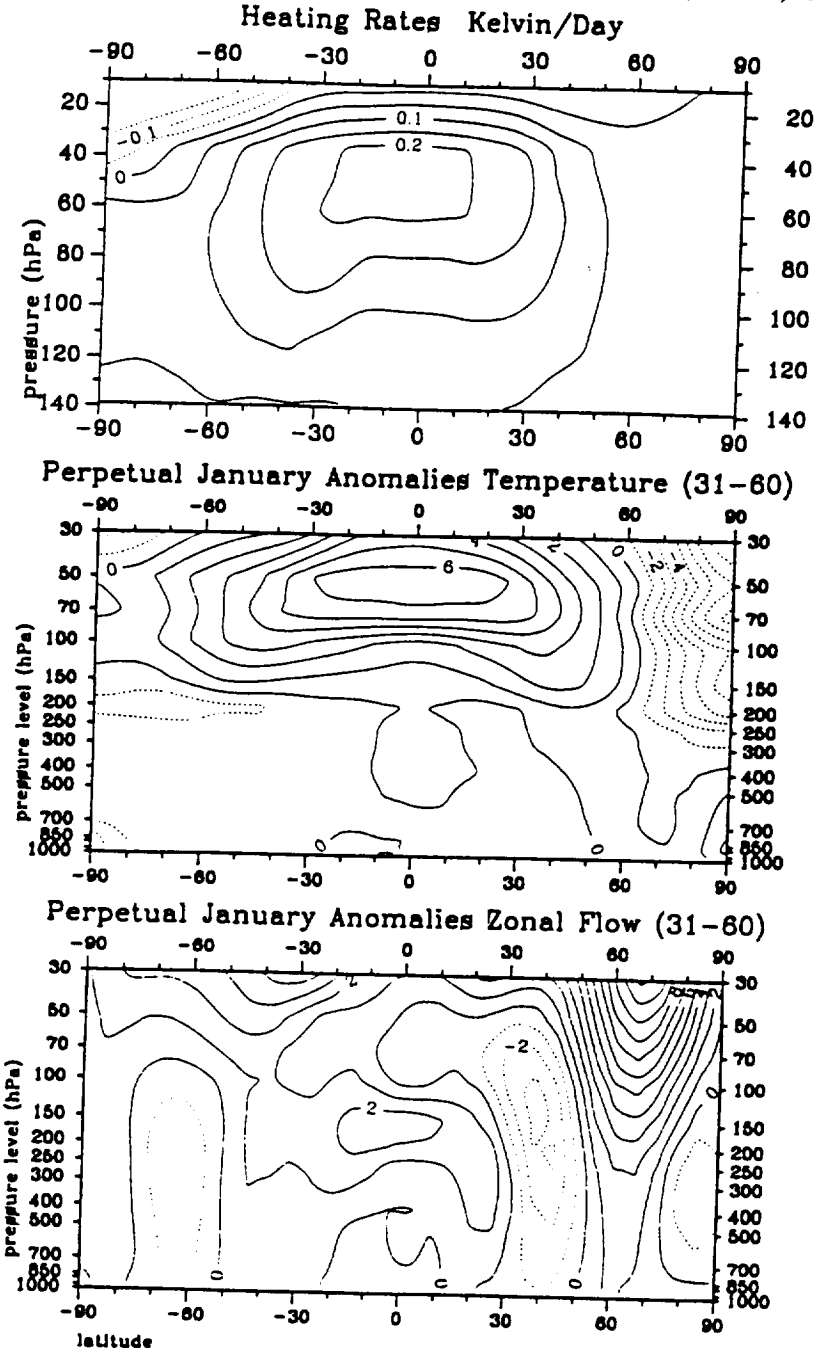

Figure 3: Cross sections of the zonal mean values of:
a) Heating rate anomalies [K/d], as determined from the radiative transfer model for January 1983 or 1992 (top).
b) Temperature anomalies [K] for Perpetual January Experiment (month 31 to 60) minus Control (middle).
c) Zonal wind anomalies [m/s] for Perpetual January Experiment minus control (month 31 to 60) (bottom).

Figure 4 gives an overview of the mean thermal and solar net radiation anomalies at earth surface as the climate model produced for three different experiments for January conditions: Perm3 is our Pinatubo experiment, SST-2 is an El Niño experiment using the observed tropical (30°N to 30°S) sea surface temperature anomalies for January 1983, and Perm6 is the combined El Niño / Pinatubo experiment which will be discussed in a succeeding paper. Anomalies of surface longwave as well as shortwave radiation are in the same order of magnitude for all experiments. In all cases there is net increase of longwave radiation in middle and high latitudes. The pure El Niño experiment only leads to a meridional shift of cloud areas and therefore to a global mean zero effect of the shortwave anomaly, while the volcanic aerosol reduces solar radiation in the order of 5 to 7 W/m^2.

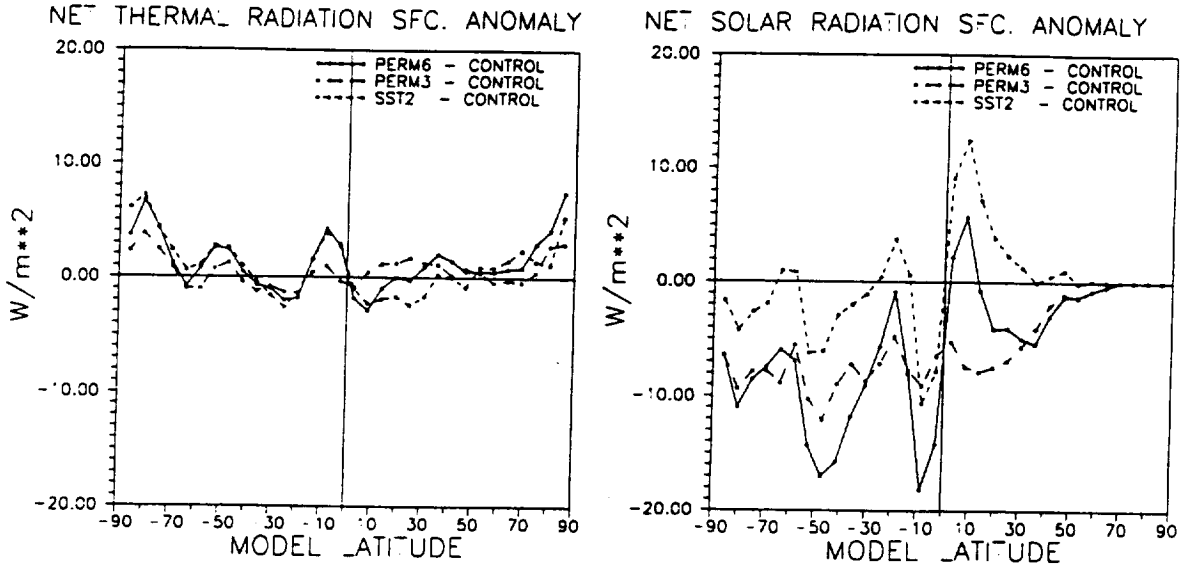

Figure 4: Net anomaly [W/m^2] at the surface for thermal (Fig. 4a) and solar (Fig. 4b) radiation for different Permanent January Experiments. PERM3 is the actual volcano experiment. SST2 is forced by tropical sea surface temperature anomalies as observed in January 1983, and PERM6 is a combination of volcanic and SST forcings.

We inspected carefully the results for possible trends in the zonal mean of temperatures and geopotential and found that there were no strong trends detectable after few months. To check for the stability of any signal, we performed analyses with different subsets consisting of 30 Januaries each. So we chose blocks of 30 succeeding Januaries and sets of randomly extracted Januaries, always excluding the first two months which show initial drift. All subsets gave the same principal patterns with only small varia-

tions in amplitudes and pattern. Here we will concentrate our discussion to the last half of the ensemble. The permanent January simulations are not independent from each other. This must be considered in the statistical tests by reducing the number of degrees of freedom. The effective number of degrees of freedom was computed for every gridpoint using the autocorrelation function. The resultant Bartels' number B (Bartels, 1935) has a global mean value of B = 1.8 (B = 1.4) for the 2m temperature (500 hPa height). This means that the effective degree of freedom is $N_{eff} = N / B$. This is consistent with the experience that the atmospheric memory is at most two weeks. Trying to stay at the conservative side of estimates, we made the assumption that every second experiment January is independent. Consequently for a set of 30 Januaries we use an effective degree of freedom of 15. This leads to a slight underestimation of the significance of the anomaly amplitudes over most parts of the globe. Only over Antarctica the Bartels' number is larger, indicating some trend of the model in this region.

Model Results

1. Stratosphere

Although the model stratosphere has only a coarse resolution, the obtained results are comparable with observations and other model studies.

The zonal mean cross section of the simulated temperature anomaly (Figure 3b) is in good qualitative agreement with the corresponding observations from December 1991 (Figure 5).Positive temperature anomalies are simulated and observed in low latitudes, and negative anomalies in the polar night region of the stratosphere. Although the heating rate anomaly is positive over the North pole (see Figure 3a), the pole cools due to a dynamic effect; because of the intensified polar stratospheric vortex the meridional (poleward) heat transport decreases. The meridional temperature gradient between the tropics and the winter pole is strengthened in the lower stratosphere. In January 1992 a minor stratospheric warming occured increasing the temperature in high northern latitudes by 5 to 6 K. Although stratospheric warmings in principle can be simulated by ECHAM2, it is not a predictable feature and is not reproduced by the model in this case.

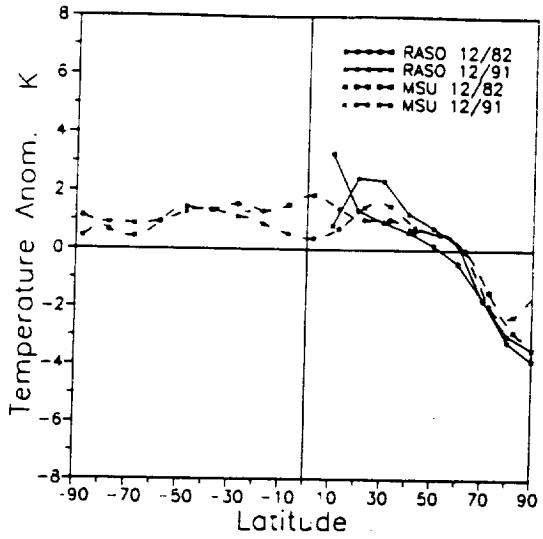

Figure 5: Observed stratospheric December temperature anomaly from the 1982-91 mean after the eruptions of El Chichón (1982) and Pinatubo (1991), data from Labitzke (radiosonde, solid lines) and Christy (MSU, broken lines).

Our results are also consistent with the study of Rind et al. (1992), who used the GISS model with an increased number of model layers (23 layers, top at 0.001 hPa). They investigated the effect of a homogenous aerosol layer of optical depth τ=0.15 on the zonal mean conditions in the middle atmosphere.

The dynamic effects in the stratosphere are primarily due to changes in the meridional temperature distribution. The mean zonal wind anomaly (Figure 3c) shows an enhanced polarnight jet in the stratosphere with anomalies up to 10 m/s. These westerly anomalies penetrate also downward into the troposphere resulting in a poleward shift of the upper tropospheric westerly jet of the northern hemisphere.

2. Troposphere

The model simulates a significant reduction of the variance of the geopotential height of the 200, 500 and 850 hPa levels over the whole North Atlantic region. This holds also for the variances of the zonal wind field and temperature (the latter mainly in the lower troposphere) for the complete set of the experiment (Figure 6) as well as for subsets. This is especially clear for the geopotential over the Azores high, over Labrador and Southern Greenland. No significant signal is detectable elsewhere applying the F-test, or the variance is increased in the experiment (Figure 6).

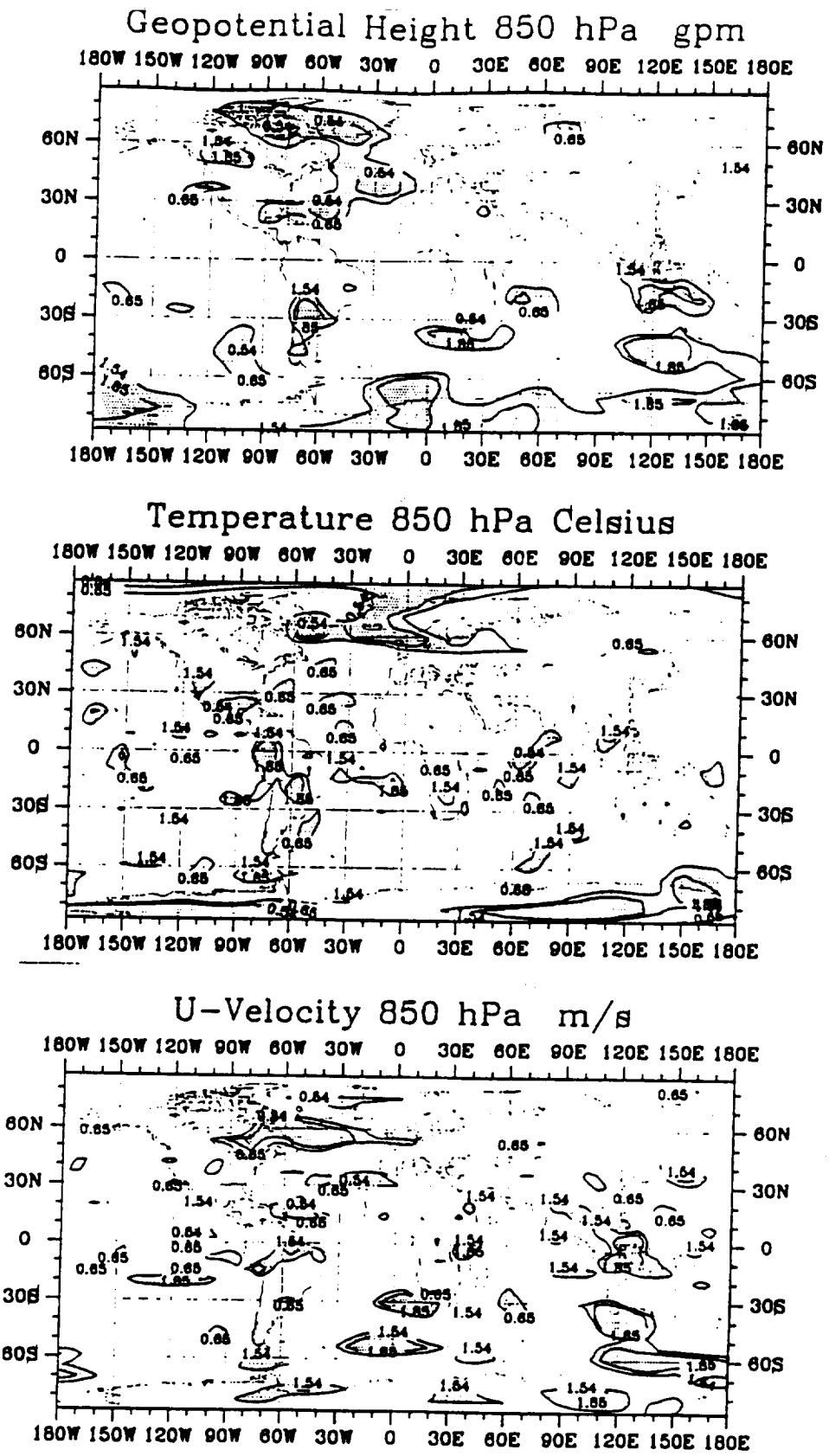

Figure 6: Changes in local variance (F-test) at the 850 hPa level for: Geopotential height (top), zonal velocity (middle), and temperature (bottom) for the Permanent January Experiment. Shading indicates significant differences between Experiment and Control. Values larger (smaller) than 1 means that the variance in the experiment is larger (smaller) than in the Control.

A local T-test was used to test for the significance of the amplitudes of the zonal wind, geopotential height and 2m-temperature anomalies in different sets of 30 experiment months. Here we will focus on the results for the Januaries 31 to 60, i.e. on the second half of the experiment. Principially, the anomaly patterns were similar in the other sets of each 30 Januaries.

In addition to the t-test, and in order to test for the difference of the distribution functions of the Control and the Experiment, a recurrency analysis (von Storch and Zwiers, 1988) was also applied to several sets of Januaries. T-test and recurrency test give comparable results, especially concerning the areas of statistically significant signals. In each set the pattern of anomalies of the geopotential heights is similar throughout the troposphere.

The largest amplitudes of the geopotential heights in all tropospheric levels occur over the North Atlantic, where the pattern indicates a northward shift of the tropospheric circulation (Figure 7). The Azores high is displaced northward by about 15° and the Icelandic low shifted towards Greenland. This pattern is significant (β=0.05) following the T-test and recurrent in all sets as well as are the negative tropical geopotential anomalies, mainly in the middle troposphere. The most prominent signal is the anticyclonic anomaly in the area of the northward shifted Azores high. Thus, the area of strongest and recurrent circulation anomalies is the North Atlantic. This holds for the whole troposphere. The structure of the anomaly patterns throughout the troposphere suggests a barotropic response. It is suggested that the interaction of the strengthened stratospheric polarnight jet with tropospheric lee effects of the Rocky Mountains is responsible for the strongest response of the circulation to the aerosol forcing over the North Atlantic. The primary effect may be a change in the stationary planetary wave pattern.

The westerlies over the North Atlantic are shifted northwards resulting in westerly wind anomalies around 60° N and easterly anomalies at 30° N (Figure 8). This pattern is again stable throughout the whole troposphere. It is also combined with a significant reduction of the variance of the zonal wind component as is obvious from the F-test. Accordingly the North Atlan-

tic centers of action shift northward.

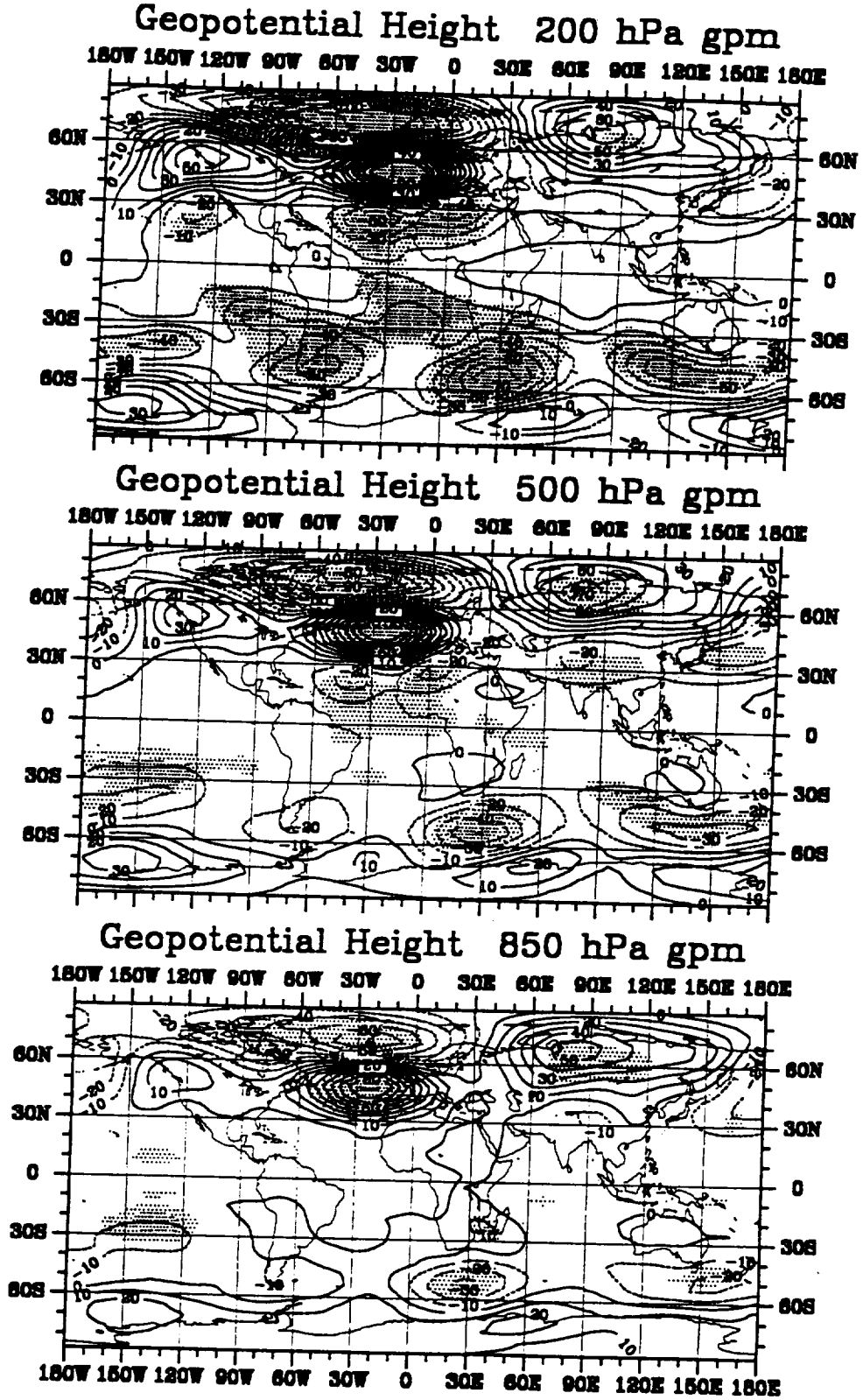

Figure 7: Anomalies of the geopotential height at different tropospheric levels. Shading indicates statistically significant (error chance 5%) differences between Control and Experiment for months 31 to 60 on the basis of a local t-test, degrees of freedom reduced to 15.

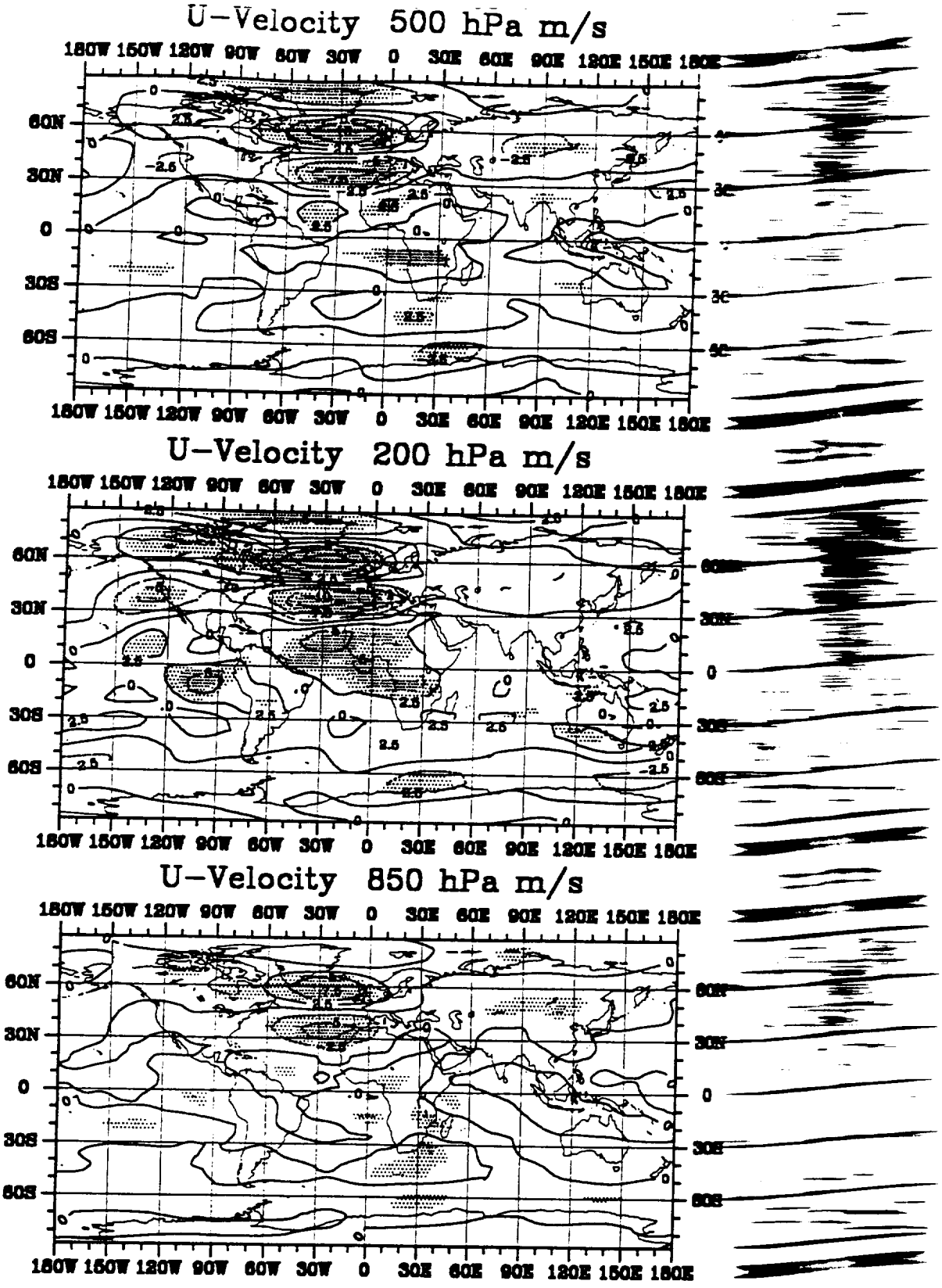

Figure 8: Anomalies of the zonal wind component at different tropospheric levels. Shading indicates statistically significant (error chance 5%) differences between Control and Experiment for months 31 to 60 on the basis of a local t-test, degrees of freedom reduced to 15.

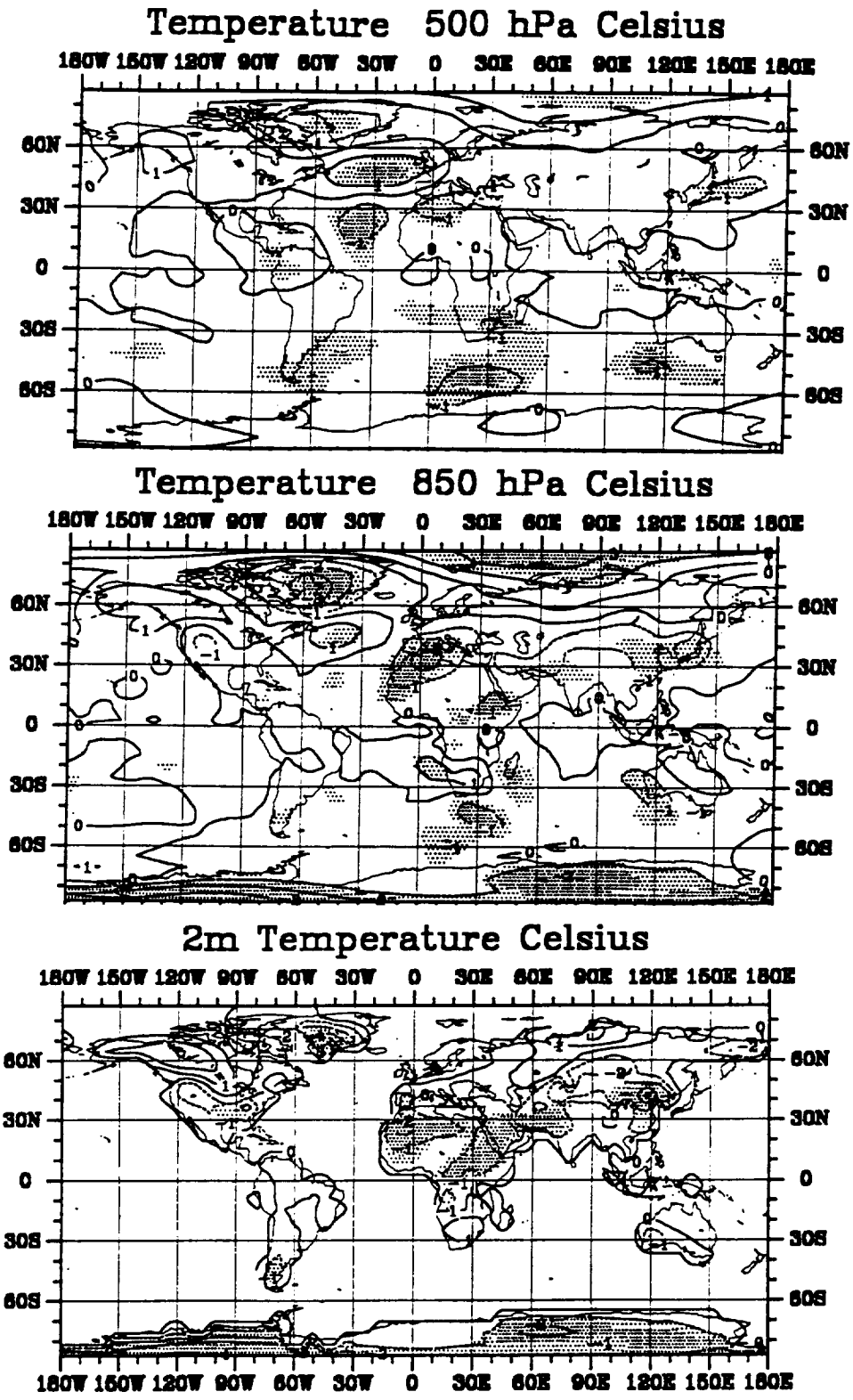

Figure 9: Anomalies of the air temperature in the lower troposphere. Shading indicates statistically significant (error chance 5%) differences between Control and Experiment for months 31 to 60 on the basis of a local t-test, degrees of freedom reduced to 15.

In the tropics, the anomalies of the zonal wind component change sign from the lower to the upper troposphere. In both sets over the eastern equatorial Pacific in the lower (upper) troposphere easterly (westerly) wind anomalies are found. This indicates a slightly strengthened Walker circulation over the eastern equatorial Pacific during winter.

The meteorological parameter which normally is of interest in connection with violent volcanic eruptions is the surface air temperature. Figure 9 (lower panel) shows the mean anomaly of this parameter, again for the last 30 Januaries of our experiment. The main features, however, are similar also for other subsets of the 60 January integration after few months of initial drift. The T-test shows a major significant area of cooling over North Africa and the Middle East, strong cooling over Greenland and parts of China. In the southern hemisphere the only significant signals are a cold southern tip of South America and Antarctic cooling. Significant warming only occurs in the Barents Sea. Here one of the model's restrictions is apparent, i.e. the fixed sea ice coverage and temperature. This in part prevents the development of positive anomalies of the 2m temperature. In the free troposphere (e.g. in 850 hPa, Figure 9, middle panel), where the surface conditions are less important and the transport processes become dominant, the warming is significant over large parts of the Arctic ocean north of Siberia and the warm anomaly reaches further south over Asia.

Tropospheric Observations

In order to compare our simulation of the impact of the Pinatubo (or an other similar volcanic eruption) stratospheric aerosol on climate with global observations data, we used the 500 hPa geopotential height anomalies as analyzed by the US National Weather Service, the satellite observed lower tropospheric temperature from the Microsounding Unit (MSU) (see Spencer and Christy, 1990), and (to a certain degree) synoptic observations collected by the Seewetteramt of the Deutscher Wetterdienst. The last data set is based on a non-uniform distribution of stations with large gaps over the oceans. This gives serious problems when the data are interpolated to a coarse map such as the T21 grid. Thus these data are used only for qualitative comparisons.

The MSU temperature data use the temperature dependence of the microwave

emission of oxygen molecules. For the tropospheric signal, calibrated MSU channel 2 (53.74 GHz) brightness temperatures are combined with a weighting function describing the vertical sensitivity to thermal emission by molecular oxygen in the atmosphere. The main part of the signal we used is from the layer between the earth surface and 400 hPa (with a peak at 700 hPa), i.e. from the lower part of the troposphere rather than from the earth surface. The spatial resolution of these observations is in the order of 10°, even though the data are published on a 2.5° grid (Spencer et al., 1990).

In order to compare with previous violent volcanic eruptions, the surface temperature data set from Jones et al. (1988) was also used (see Robock and Mao, 1992 submitted).

An inspection of the mean December 1991 through February 1992 500 hPa height anomaly (Figure 10) shows some similarity between our simulation and observed anomalies: The strongest anomalies occur in the Atlantic region.

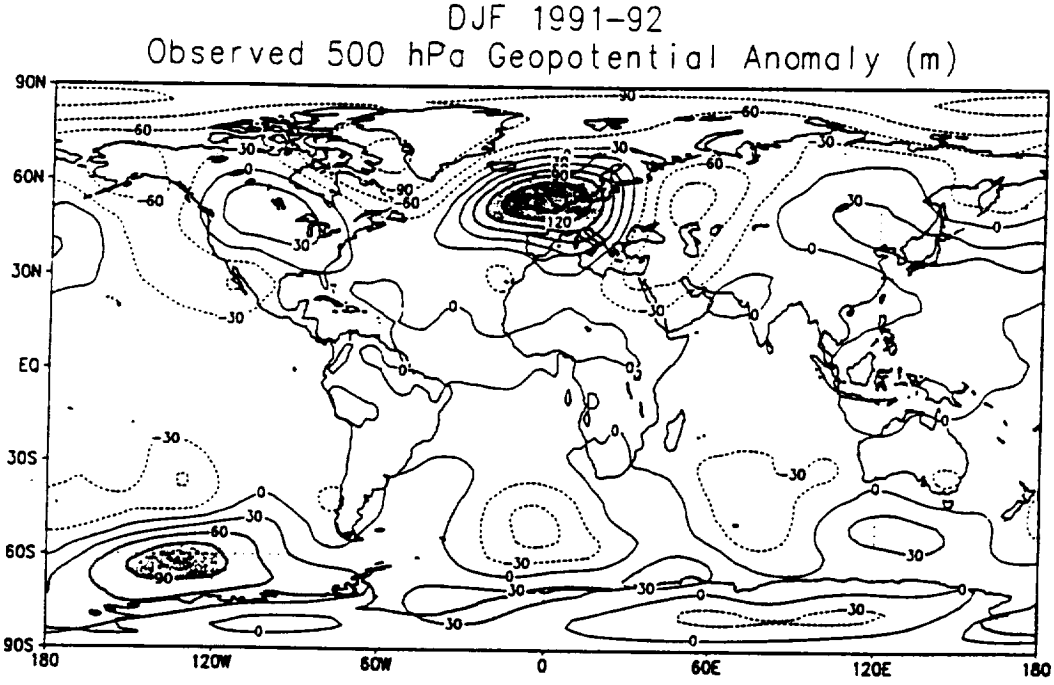

Figure 10: Anomaly of the 500 hPa geopotential height as analyzed by the US NWS, mean of December 1991 through February 1992. Anomalies calculated from mean 1982-1990.

The simulated anomalies are generally weaker than the observed ones and a tendency to a westward displacement is characteristic. Such zonal (westward) displacements (compared with observations) of the mean circulation features are common in low resolution GCMs, resulting mainly from the smooth orographic representation (Sausen 1992, pers. comm.). The negative anomaly over Greenland exists in both fields (for the simulated anomaly see Figure 6), while the observed center of the positive geopotential anomaly is shifted eastwards to England. Both, in the observations and in the simulation, a trough develops over Eastern Europe / Western Asia, which also has a more westerly position than in the observations. The pattern anomaly correlation (Table 1) is between 0.37 for the globe and 0.40 for the northern hemisphere if we use the mean pattern of the experiments 03-60. As stated above, subsets have shown the same patterns. This means that only about 15% of the total North hemispheric observed spatial variance of the 500 hPa field of the middle troposphere in winter 1991-92 can be explained by the volcanic impact alone. Much better results we get for the western hemisphere (180°W to 0°) where this value can be improved to 49% (r=0.70).

Table 1: Pattern correlation coefficients (area weighted, multiplied by 100) between observed and simulated meteorological fields. A 1:1 correlation means that no spatial shift is allowed, "optimal" correlation allows for 2 gridpoints shift in all directions to get a best fit. All fields were interpolated to the T21 grid before being analyzed. Mean of the experiments 03-60 used.

Parameter	global	N-hemisph.	90°W-90°E	0°-180°E	0°-180°W
MSU-Temp.					
1:1	18	57	39	54	60
optimal	29	57	62	56	63
500 hPa					
1:1	35	39	1	-29	68
optimal	37	40	41	-46	70

Over Siberia the patterns of 500 hPa geopotential height anomalies do not agree well because of a simulated high over North Siberia which is not observed in winter 1991/92.

For the lower tropospheric temperature (Figure 11), reasonable agreement between simulations and observations in winter 1991-92 is found for the

northern hemisphere again. The "optimal" pattern correlations are between τ=0.56 and τ=0.63 for different subareas of the Northern hemisphere (Table 1), resulting in τ=0.57 for the whole northern hemisphere. This means that about 35 to 40% of the total spatial variance of the observed 2m temperature can be explained alone by the volcanic forcing. The model reproduced especially well the cooling over Greenland and North Africa. Some of the warming of the middle and high latitudes of the northern continents, which is seen in both patterns, is also modelled at the right place, although not significant with respect to the amplitude because of the high variability of the temperature in these latitudes in the control run.

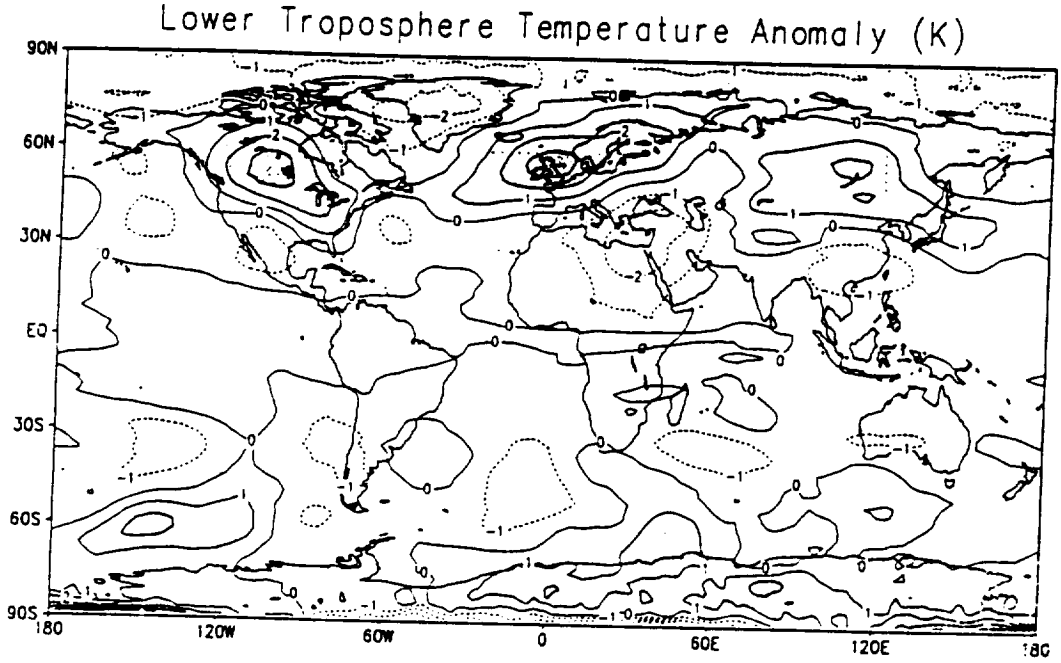

Figure 11: Anomaly of the air temperature near surface [K] as observed December 1991 through February 1992 from MSU satellite data (Spencer and Christy, 1991). Anomalies calculated from mean for 1982-1990.

The good agreement between the model simulation and the observations in winter 19991/92 still could be coincidental. This might be excluded if similar anomaly patterns evolved after other volcanic eruptions as well.

An examination of the near surface temperature data set from Jones et al. (1988 and 1991, updated, Jones, personal comm.) after the twelve most violent volcanic eruptions of the last century (Figure 12) also shows good agreement with our simulations. For the six tropical volcanoes (Krakatau, Sta Maria, Agung, Fuego, El Chichón and Pinatubo) the anomalies are for the

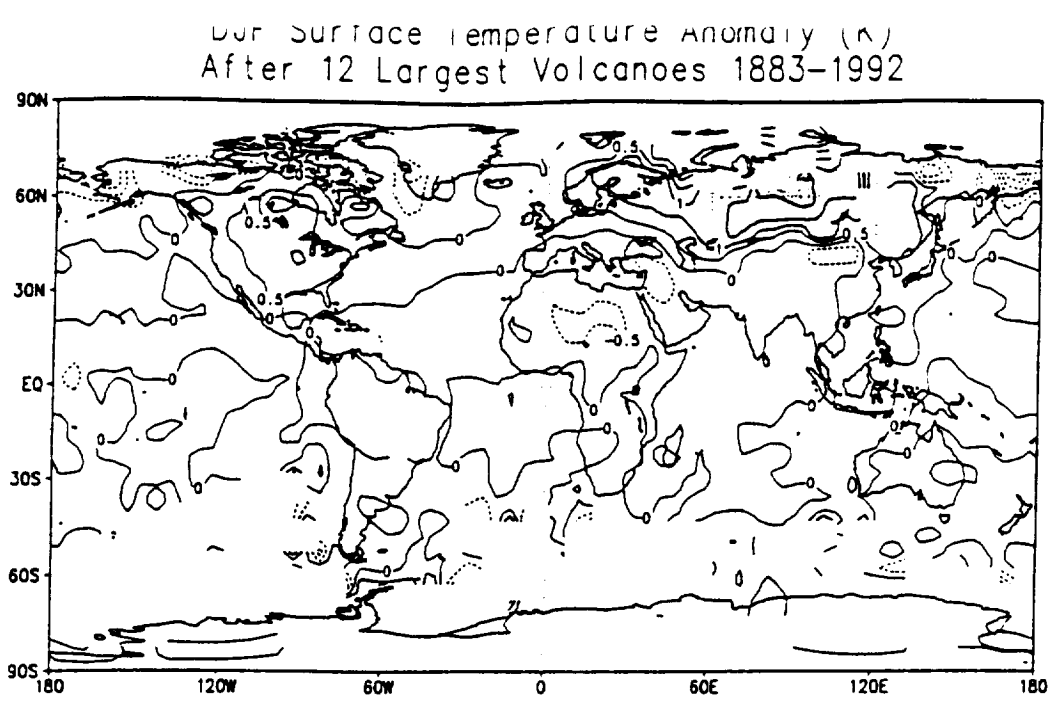

Figure 12: Observed December through February mean temperature anomaly after the twelve largest volcanic eruptions of the last century (Data from Jones, 1988, updated, Jones, pers. comm.).

following boreal winter, for the six high latitude volcanoes (Novarupta, Tarawera, Bandai, Ksudach, Cerro Azul and Bezymianny) anomalies are for the second winter after the eruption to allow time for the aerosols to reach the tropical stratosphere. The anomalies are calculated from the 1951 to 1980 means differences from low pass (cut-off 10 years) filtered data. The pattern after every volcano is virtually the same as the mean effect shown in Figure 12, except some differences over North America for winters with and without El Niños. The best pattern correlation between the composite signal of post eruption winter temperatures and our simulation is found for the sector between 90°W and 90°E on the Northern hemisphere (τ=0.35). There is a zero pattern correlation for the western half of the North hemisphere and only τ=0.21 for the eastern half.

Conclusions

The perpetual January GCM simulation has shown that the stratospheric aerosol produced by a violent and sulfur-rich volcanic eruption can alter the stratospheric and tropospheric climate conditions significantly. Using the

"anomaly forcing" technique the stratospheric forcing due to the aerosol (which is not included in the original GCM) can be simulated in accordance with other model simulations and observations. The stratospheric winter signal can be described as a significant warming of the aerosol containing layers in the tropics and midlatitudes due to absorption of radiative energy. This warming increases the poleward meridional temperature gradient, leads to an increased polar night jet, reduced meridional heat transport and therefore a cooling tendency in the stratosphere over the winter pole.

In this study the tropospheric signal was found to be meridionally non-uniform. It is strongest over the North Atlantic and consistsof enhanced westwinds over high latitudes (around 60°N), strengthened zonal heat and moisture transport in higher latitudes and a northward shift of the Azores high. The areas of strongest anomalies also show significantly reduced variance of the parameters.

A temperature anomaly field was found in the lower troposphere, which (in the main features) is very similar to observations during the winter 1991-92 . Similar anomalies were observed also during other post volcano winters. There is a significant cooling over Greenland and North Africa / Middle East. In agreement with observations some warming tendency with a maximum amplitude of about 2 K is seen in the mean results over North America and northern Eurasia. This positive temperature anomaly can not be proved to be statistically significant because of the large natural variability of surface temperature in these latitudes. This warm anomaly is supported by observations following historic eruptions (Robock and Mao 1992) and it determines the high pattern correlation found between simulation and observations.

The simulated and observed temperature anomalies following a violent volcanic eruption in part contradict the findings based on linear multiple regression analysis (Cress and Schönwiese 1991) and energy balance models (Robock 1984). The results underline the importance of nonlinear and dynamic responses of the atmosphere to external forcing.

ACKNOWLEDGMENTS: We thank John Christy, Phil Jones and Karin Labitzke for providing the temperature data. We are grateful to M. Grunert for preparing Figure 1, to Jiaoping Mao for producing the analyses in Figure 12 and to Brian Doty for the GrADS software for Figures 10 to 12. We thank Huug van den Dool and John Janowiak for the 500 hPa data. Data are from the Climate Analysis Center of the National Meteorological Center of NOAA. Comments of Lennart Bengtsson and Mojib Latif on a first version of the manuscript helped clarify the presentation. This work was partially supported by the Bundesministerium für Forschung und Technologie (No. 07-KFT-86/2), NSF grant ATM-8920590 and NASA grant NAG 5-1835.

Literature:

Bakan,S., A. Chlond, U. Cubasch, J. Feichter, H. Graf, H. Grassl, K. Hasselmann, I. Kirchner, M. Latif, E. Roeckner, R. Sausen, U. Schlese, D. Schriever, I. Schult, U. Schumann, F. Sielmann and W. Welke, 1991: Climate response to smoke from the burning oil wells in Kuwait. Nature, 351, 367-371

Bakan,S., 1982: Strahlungsgetriebene Zellularkonvektion in Schichtwolken. Dissertation, Univ. Hamburg, 99 S.

Bartels,J., 1935: Random fluctuations, persistence, and quasipersistence in geophysical and cosmical periodicities. Terrestr. Magnetism atmospher. Electr., 40, 1-60

Boville,B.A., 1986: The influence of the polar night jet on the tropospheric circulation in a GCM. Journ. Atmosph. Sci., 41, 1132-1142

Bluth,G.J.S.; S.D.Doiron; A.J.Krueger; L.S. Walter and C.C.Schnetzler, 1991: Global Tracking of the SO2 clouds from the June, 1991 Mount Pinatubo Eruptions, Geophys.Res.Lett., 19, Jan. 1992

Cress, A. und Ch.-D. Schönwiese, 1990: Vulkanische Einflüsse auf die bodennahe und stratosphärische Lufttemperatur der Erde. Ber. Inst. f. Meteorologie und Geophysik Univ. Frankfurt/Main, Nr. 82, 148 S.

Geller,M.A. and J.C. Alpert, 1980: Planetary wave coupling between the troposphere and the middle atmosphere as a possible sun-weather mechanism. J. Atmos. Sci., 37, 1197-1215

Graf,H.-F., 1986: On El Niño/Southern Oscillation and northern hemispheric temperature. Gerl. Beitr. Geophys. 95, 63-75

Graf,H.-F., 1992: Arctic radiation deficit and climate variability. Climate Dynamics, 7, 19-28

Groismann,P.Y., 1985: Regional climatic consequences of volcanic eruptions. Meteorology and Hydrology, No.4, 39-45. [in Russian]

Groisman, P.Y., 1992: Possible regional consequences of the Pinatubo eruption: an empirical approach. Geophys. Res. Lett., 19, 1603-1606

Hansen,J.; Lacis,A.; Ruedy,R. and M.Sato, 1992: Potential climate impact of Mount Pinatubo eruption. Geophys.Res.Lett., 19, 215-218

Jäger,H., 1992: The Pinatubo cloud observed by Lidar over Garmisch-Partenkirchen. Geophys. Res. Lett. 19, 191-194

Jones, P.D., 1988: Hemispheric surface air temperature variations: recent trends and an update to 1987. J. Climate,1, 654-660

Jones, P.D., T.M.L. Wigley, C.K. Folland, D.E. Parker, J.K. An-

gell, S. Lebedeff and J.E. Hansen, 1988: Evidence for global warming in the past decade. Nature, 332, 790

Lacis, A., J. Hansen and M. Sato, 1992: Climate forcing by stratospheric aerosols. Geophys. Res. lett. ,19, 1607-1610

Lough,J.M., H.C. Fritts, 1987: An assessment of the possible effects of volcanic eruptions on North American climate using tree-ring data, 1602-1900 A.D., Climatic Change, 10, 219-239.

Rind, D., N.K. Balachandran and R. Suozzo, 1992: Climate change and the middle atmosphere. Part II: The impact of volcanic aerosols. J. Climate, 5, 189-208

Robock,A.D., 1984: Climate model simulations of the El Chichón eruption. Geofisica Internacional, 23, 403-414

Robock, A.D., in Greenhouse-Gas-Induced Climatic Change: A Critical Appraisal of Simulations and Observations (ed. M.E. Schlesinger), 429-444, (Elsevier, Amsterdam,1991).

Robock, A. and J. Mao, 1992: Winter warming from large volcanic eruptions. Submitted to Geophys. Res. Lett.

Roeckner, E., K. Arpe, L. Bengtsson, S. Brinkop, L. Dümenil, M. Esch, E. Kirk, F. Lunkeit, M. Ponater, B. Rockel, R. Sausen, U. Schlese, S. Schubert and M. Windelband, 1992: Simulation of the present-day climate with the ECHAM model: Impact of model physics and resolution. MPI Report No. 95

Schmitz,G. and N. Grieger, 1980: Model calculations of the structure of planetary waves in the upper troposphere and lower stratosphere as a function of the wind field in the upper stratosphere. Tellus, 32, 207-214

Schult,I., 1991: Bildung und Transport von Aerosolteilchen in der Stratosphäre und ihre Bedeutung für den Strahlungshaushalt. Examensarbeit Nr. 11, Max-Planck-Institut für Meteorologie Hamburg

Spencer,R.W.,J.R. Christy, and N.C. Grody 1990: Global atmospheric temperature monitoring with satellite microwave measurements: Method and results 1979-84, J. Climate, 3, 1111-1128.

Spencer,R.W. and J.R. Christy, 1991: General Temperature update to 31 October 1991. NASA Headquarters, Washington, (pers. comm.)

Storch, H. von, F. W. Zwiers, 1988: Recurrenceanalysis of climate sensitivity experiments. J. Climate, 1, 157-171.

MPI Report-Reference: *Reprinte

Report No. 1-60	Please order the reference list from the MPI Hamburg
Report No. 61 March 1991	**Three-Dimensional Simulation of Cloud Street Development during a Cold Air Outbreak** Andreas Chlond
Report No. 62 April 1991	**Modelling the low-frequency sea surface temperature variability in the Northern Pacific** Ute Luksch, Hans von Storch *Journal of Climate, 1992
Report No. 63 May 1991	**How much predictive skill is contained in the thermal structure of an OGCM** Mojib Latif, Nicholas E. Graham * Journal of Phys. Oceanography
Report No. 64 June 1991	**Downscaling of Global Climate Change Estimates to Regional Scales: An Application to Iberian Rainfall in Wintertime** Hans von Storch, Eduardo Zorita, Ulrich Cubasch *Journal of Climate, 1992
Report No. 65 June 1991	**Southern Ocean Sea-Ice Simulations forced with operationally derived Atmospheric Analyses Data** Achim Stössel
Report No. 66 June 1991	**The Phase of 30- to 60-Day Oscillation and the Genesis of Tropical Cyclones in the Western Pacific** Hans von Storch, Ann Smallegange
Report No. 67 July 1991	**Time-Dependent Greenhouse Warming Computations with a Coupled Ocean-Atmosphere Model** Ulrich Cubasch, Klaus Hasselmann, Heinke Höck, Ernst Maier-Reimer, Uwe Mikolajewicz, Benjamin D. Santer, Robert Sausen
Report No. 68 July 1991	**On the sensitivity of the Global Ocean Circulation to Changes in the Surface Heat Flux Forcing** Ernst Maier-Reimer, Uwe Mikolajewicz, Klaus Hasselmann
Report No. 69 August 1991	**Acoustic Detection of Greenhouse-Induced Climate Changes in the Presence of Natural Variability** Uwe Mikolajewicz, Ernst Maier-Reimer, Tim P. Barnett
Report No. 70 September 1991	**The Effect of a Regional Increase in Ocean Surface Roughness on the Tropospheric Circulation: A GCM Experiment** Uwe Ulbrich, Gerd Bürger, Dierk Schriever, Hans von Storch, Susanne L. Weber, Gerhard Schmitz
Report No. 71 September 1991	**A differential absorption lidar system for high resolution water vapor measurements in the troposphere** Jens Bösenberg
Report No. 72 September 1991	**Coupling an Ocean Wave Model to an Atmospheric General Circulation Model** Susanne L. Weber, Hans von Storch, Petro Viterbo, Liana Zambresky
Report No. 73 September 1991	**Climate Variability in a Coupled GCM. Part 1: The Tropical Pacific** Mojib Latif, Andreas Sterl, Ernst Maier-Reimer, Martina M. Junge

in

MPI-Report-Reference: *Reprinted in

Report No. 74 October 1991	**On the Space-Time Structure on ENSO** Mojib Latif, Andreas Sterl, Ernst Maier-Reimer
Report No. 75 October 1991	**On the Navigation of Polar Orbiting Meteorological Scatellites** Jaruslav Klokocnik, Peter Schlüssel, Jan Kostelecky, Hartmut Grassl
Report No. 76 January 1992	**A Hybrid Coupled Tropical Atmosphere Ocean Model: Sensitivities and Hindcast Skill** Richard Kleeman, Mojib Latif, Moritz Flügel
Report No. 77 January 1992	**A Direct Mathematical Approach to Optimize the Age-Depth Relation of Deep-Sea Sediment Cores** Wolfgang Brüggemann
Report No. 78 January 1992	**The Joint Normal Modes of the coupled Atmosphere-Ocean System observed from 1967 to 1986** Jin-Song Xu
Report No. 79 January 1992	**Orbital tuning of marine sedimentary cores: An automatic procedure based on a general linear model** Björn Grieger
Report No. 80 March 1992	**Application of ocean models for the interpretation of AGCM experiments on the climate of the last glacial maximum** Michael Lautenschlager, Uwe Mikolajewicz, Ernst Maier-Reimer, Christoph Heinze
Report No. 81 March 1992	**Normal Modes of the Atmosphere as estimated by Principal Oscillation Patterns and derived from Quasi-Geostrophic Theory** Reiner Schnur, Gerhard Schmitz, Norbert Grieger, Hans von Storch
Report No. 82 May 1992	**On regional surface fluxes over partly forested areas** Martin Claussen, Wim Klaassen
Report No. 83 May 1992	**On the cold start problem in transient simulations with coupled atmosphere-ocean models** Klaus Hasselmann, Robert Sausen, Ernst Maier-Reimer, Reinhard Voss
Report No. 84 May 1992	**Iron fertilization of the Austral Ocean - a model assessment** Katharina D. Kurz, Ernst Maier-Reimer *Global Biogeochemical Cycles
Report No. 85 June 1992	**A snow cover model for global climatic simulations** Bettina Loth, Hans F. Graf, Josef M. Oberhuber
Report No. 86 June 1992	**Complex principal oscillation pattern analysis** Gerd Bürger
Report No. 87 August 1992	**Scale aggregation in semi-smooth flow** Martin Claussen
Report No. 88 August 1992	**Optimal fingerprints for the detection of time dependent climate change** Klaus Hasselmann
Report No. 89 September 1992	**Biomes computed from simulated climatologies** Martin Claussen, Monika Esch

MPI-Report-Reference: *Reprinted in

Report No. 90
September 1992

New generation of radiation budget measurements from space and their use in climate modelling and diagnostic studies
L.Dümenil, E. Raschke

Report No. 91
September 1992

Modal structure of variations in the tropic climate system Part I: Observations
Mojib Latif, Timothy P. Barnett, Keisuke Mizuno

Report No. 92
October 1992

The Köppen Climate Classification as a Diagnostic Tool for General Circulation Models
Ulrike Lohmann, Robert Sausen, Lennart Bengtsson, Ulrich Cubasch Jan Perlwitz, Erich Roeckner

Report No. 93
October 1992

Simulation of the present-day climate with the ECHAM model: Impact of model physics and resolution
E. Roeckner, K. Arpe, L. Bengtsson, S. Brinkop, L. Dümenil, M. Esch, E. Kirk, F. Lunkeit, M. Ponater, B. Rockel, R. Sausen, U. Schlese, S. Schubert, M. Windelband

Report No. 94
October 1992

Pinatubo Eruption Winter Climate Effects: Model Versus Observations
Hans-F. Graf, Ingo Kirchner, Alan Robock, Ingrid Schult